BNL-216245-2020-JAAM

Anisotropic magnetocaloric effect and critical behavior in CrSbSe3

Y. Liu

To be published in "PHYSICAL REVIEW B"

July 2020

Condensed Matter Physics and Materials Science Department

Brookhaven National Laboratory

U.S. Department of Energy

USDOE Office of Science (SC), Basic Energy Sciences (BES) (SC-22)

Notice: This manuscript has been authored by employees of Brookhaven Science Associates, LLC under Contract No. DE-SC0012704 with the U.S. Department of Energy. The publisher by accepting the manuscript for publication acknowledges that the United States Government retains a non-exclusive, paid-up, irrevocable, world-wide license to publish or reproduce the published form of this manuscript, or allow others to do so, for United States Government purposes.

DISCLAIMER

This report was prepared as an account of work sponsored by an agency of the United States Government. Neither the United States Government nor any agency thereof, nor any of their employees, nor any of their contractors, subcontractors, or their employees, makes any warranty, express or implied, or assumes any legal liability or responsibility for the accuracy, completeness, or any third party's use or the results of such use of any information, apparatus, product, or process disclosed, or represents that its use would not infringe privately owned rights. Reference herein to any specific commercial product, process, or service by trade name, trademark, manufacturer, or otherwise, does not necessarily constitute or imply its endorsement, recommendation, or favoring by the United States Government or any agency thereof or its contractors or subcontractors. The views and opinions of authors expressed herein do not necessarily state or reflect those of the United States Government or any agency thereof.

Anisotropic magnetocaloric effect and critical behavior in $CrSbSe_3$

Yu Liu (刘育),[1] Zhixiang Hu (胡之翔),[1,2] and C. Petrovic[1,2]
[1] *Condensed Matter Physics and Materials Science Department, Brookhaven National Laboratory, Upton, New York 11973, USA*
[2] *Materials Science and Chemical Engineering Department, Stony Brook University, Stony Brook, New York 11790, USA*
(Dated: June 14, 2020)

We report anisotropic magnetocaloric effect and critical behavior in quasi-one-dimensional ferromagnetic $CrSbSe_3$ single crystal. The maximum magnetic entropy change $-\Delta S_M^{max}$ is 2.16 J kg^{-1} K^{-1} for easy a axis (2.03 J kg^{-1} K^{-1} for hard b axis) and the relative cooling power RCP is 163.1 J kg^{-1} for easy a axis (142.1 J kg^{-1} for hard b axis) near T_c with a magnetic field change of 50 kOe. The magnetocrystalline anisotropy constant K_u is estimated to be 148.5 kJ m^{-3} at 10 K, decreasing to 39.4 kJ m^{-3} at 70 K. The rescaled $\Delta S_M(T,H)$ curves along all three axes collapse onto a universal curve, respectively, confirming the second order ferromagnetic transition. Further critical behavior analysis around $T_c \sim 70$ K gives that the critical exponents $\beta = 0.26(1)$, $\gamma = 1.32(2)$, and $\delta = 6.17(9)$ for $H \parallel a$, while $\beta = 0.28(2)$, $\gamma = 1.02(1)$, and $\delta = 4.14(16)$ for $H \parallel b$. The determined critical exponents suggest that the anisotropic magnetic coupling in $CrSbSe_3$ is strongly dependent on orientations of the applied magnetic field.

I. INTRODUCTION

Low-dimensional ferromagnetic (FM) semiconductors, holding both ferromagnetism and semiconducting character, form the basis for nano-spintronics application. Recently, the two-dimensional (2D) CrI_3 and $Cr_2Ge_2Te_6$ have attracted much attention since the discovery of intrinsic 2D magnetism in mono- and few-layer devices.[1–4] Intrinsic magnetic order is not allowed at finite temperature in low-dimensional isotropic Heisenberg model by the Mermin-Wagner theorem,[5] however, a large magnetocrystalline anisotropy removes this restriction, for instance, the presence of a magnetically ordered state in the 2D Ising model. The enhanced fluctuations in 2D limit make symmetry-breaking order unsustainable, however by gapping the low-energy modes through the introduction of anisotropy, order could be established by providing stabilization of long-range correlations in 2D limit. Given the reduced crystal symmetry in low-dimensional magnets, an intrinsic magnetocrystalline anisotropy can be expected and points to possible long-range magnetic order in atomic-thin limit.

In ternary chromium trichalcogenides, $Cr(Sb,Ga)X_3$ (X = S, Se, Te) displays a pseudo-one-dimensional crystal structure. This is different from $Cr(Si,Ge)Te_3$ that features layered structure and a van der Waals bonds along the c-axis. In $Cr(Sb,Ga)X_3$, the CrX_6 octahedra form infinite, edge-sharing, double rutile chains. The neighboring chains are linked by Sb or Ga atoms. The FM semiconductor $CrSbSe_3$ has attracted considerable attention.[6–9] A band gap of 0.7 eV was determined by resistivity and optical measurements.[8] The Cr in $CrSbSe_3$ exhibits a high spin state with $S = 3/2$, and orders ferromagnetically below the Curie temperature T_c of 71 K.[8] FM state in $CrSbSe_3$ is fairly anisotropic with the a axis being the easy axis and the b axis being the hard axis. The critical analysis where magnetic field was applied along the a axis suggests that the ferromagnetism in $CrSbSe_3$ cannot be simply described by the mean-field theory.[10,11] This invites the detailed investigation on its anisotropic critical behavior.

The magnetocaloric effect (MCE) can give additional insight into the magnetic properties, and it could be also used to assess magnetic refrigeration potential.[12–20] Bulk $CrSiTe_3$ exhibits anisotropic entropy change ($-\Delta S_M^{max}$) with the values of 5.05 and 4.9 J kg^{-1} K^{-1} at 50 kOe for out-of-plane and in-plane fields, respectively, with the magnetocrystalline anisotropy constant K_u of 65 kJ m^{-3} at 5 K.[14] The values of $-\Delta S_M^{max}$ are about 4.24 J kg^{-1} K^{-1} (out-of-plane) and 2.68 J kg^{-1} K^{-1} (in-plane) at 50 kOe for CrI_3 with a much larger K_u of 300 ± 50 kJ m^{-3} at 5 K.[21] The large magnetocrystalline anisotropy is important in preserving FM in the 2D limit.

In the present work we investigate the anisotropic magnetic properties of pseudo-one-dimensional $CrSbSe_3$ single crystals. The magnetocrystalline anisotropy constant K_u is strongly temperature-dependent.It takes a value of $\sim$ 148.5 kJ m^{-3} at 10 K and monotonically decreases to 39.4 kJ m^{-3} at 70 K for the hard b axis. The K_u of $CrSbSe_3$ is much larger than that of $Cr_2(Si,Ge)_2Te_6$ but comparable with that of $Cr(Br,I)_3$. This results in anisotropic magnetic entropy change $\Delta S_M(T,H)$ and relative cooling power (RCP), as well as in magnetic critical exponents β, γ, and δ that point to the nature of the phase transition. The anisotropic magnetic coupling of $CrSbSe_3$ is strongly dependent on orientations of the applied magnetic field, providing an excellent platform for further theoretical studies of low-dimensional magnetism.

II. EXPERIMENTAL DETAILS

$CrSbSe_3$ single crystals were fabricated by the self-flux technique starting from an intimate mixture of raw materials Cr (99.95%, Alfa Aesar) powder, Sb (99.999%, Alfa Aesar) pieces, and Se (99.999%, Alfa Aesar) pieces with

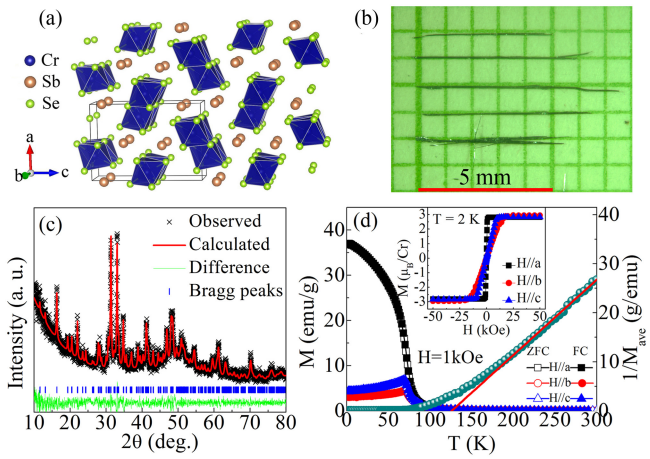

FIG. 1. (Color online). (a) Crystal structure of $CrSbSe_3$ and (b) representative single crystals on a millimeter-grid paper. (c) Powder x-ray diffraction (XRD) pattern of $CrSbSe_3$. (d) Temperature-dependent magnetization M(T) measured in H = 1 kOe with zero field cooling (ZFC) and field cooling (FC) modes along all three axes (left axis) and inverse average magnetization $1/M_{ave} = 3/(M_a + M_b + M_c)$ (right axis) fitted by the Curie-Weiss law. Inset shows the field-dependent magnetization $M(H)$ at 2 K.

a molar ratio of 7 : 33 : 60. The starting materials were sealed in an evacuated quartz tube and then heated to 800 °C and slowly cooled to 680 °C with a rate of 2 °C/h. Needle-like single crystals with lateral dimensions up to several millimeters can be obtained. The element analysis was performed using an energy-dispersive x-ray spectroscopy in a JEOL LSM-6500 scanning electron microscope (SEM), confirming a stoichiometric $CrSbSe_3$ single crystal. The powder x-ray diffraction (XRD) data were taken with Cu K_α ($\lambda = 0.15418$ nm) radiation of Rigaku Miniflex powder diffractometer. The anisotropy of magnetic properties were measured by using one single crystal with mass of 0.32 mg and characterized by the magnetic property measurement system (MPMS-XL5, Quantum Design). The applied field (H_a) was corrected as $H = H_a - NM$, where M is the measured magnetization and N is the demagnetization factor. The corrected H was used for the analysis of magnetic entropy change and critical behavior.

III. RESULTS AND DISCUSSIONS

Figure 1(a) displays the $CrSbSe_3$ crystal structure. The material crystalizes in an orthorhombic lattice with the space group of *Pnma*. That is a pseudo-one-dimensional structure with double rutile chains of $CrSe_6$ octahedra that are aligned parallel to the b axis. As shown in Fig. 1(b), the b axis is along the long crystal dimension in single crystals. Within the double chain, the Cr cations form an edge-sharing triangular arrangement, while the Sb atoms link the adjacent chains. In the powder XRD pattern [Fig. 1(c)], all peaks can be well indexed by the orthorhombic structure (space group *Pnma*) with lattice parameters $a = 9.121(2)$ Å, $b = 3.785(2)$ Å and $c = 13.383(2)$ Å, in good agreement with previous report.[8]

Figure 1(d) shows the temperature dependence of magnetization $M(T)$ along all three axes measured at $H = 1$ kOe. There is no bifurcation seen between the zero-field-cooling (ZFC) and field-cooling (FC) curves, indicating the high quality of single crystal. The $M(T)$ curves are nearly isotropic at high temperature but show an obvious anisotropic magnetic response for field applied along different axes at low temperature. For $H \parallel a$, a rapid increase near 70 K in $M(T)$ on cooling corresponds well to the reported paramagnetic (PM) to FM transition.[8] For $H \parallel b$ and $H \parallel c$, an anomalous peak feature is observed, which is also seen in $Cr_2(Si,Ge)_2Te_6$ and $Cr(Br,I)_3$ with a large magnetocrystalline anisotropy.[22–24] The inverse average magnetization $1/M_{ave} = 3/(M_a + M_b + M_c)$ can be well fitted from 200 to 300 K by using the Curie-Weiss law, which generates an effective moment of 4.6(1) μ_B/Cr and a positive Weiss temperature of 125(1) K, in line with the values reported for $CrSbSe_3$ polycrystals.[6,7] The anisotropic magnetization isotherms measured at $T = 2$ K [inset in Fig. 1(d)] show a similar saturated magnetization M_s at 3 μ_B/Cr, consistent with expectation of $S = 3/2$ for Cr^{3+}, but different saturated fields H_s of 1 kOe, 18 kOe, and 12 kOe for a, b, and c axis, respectively, close to the values in the previous reports.[8,9]

To further characterize the anisotropic magnetic properties of $CrSbSe_3$, the isothermal magnetization with field up to 50 kOe applied along each axis from 10 to 100 K are presented in Figs. 2(a)-2(c). At high temperature, the curves have linear field dependence. With decreasing temperature, the curves bend with negative curvatures, indicating dominant FM interaction. Based on the classical thermodynamics and Maxwell's relation, the magnetic entropy change $\Delta S_M(T, H)$ is given by:[25,26]

$$\Delta S_M = \int_0^H [\frac{\partial S(T,H)}{\partial H}]_T dH = \int_0^H [\frac{\partial M(T,H)}{\partial T}]_H dH, \quad (1)$$

where $[\partial S(T,H)/\partial H]_T = [\partial M(T,H)\partial T]_H$ is based on the Maxwell's relation. For magnetization measured at small temperature and field intervals,

$$\Delta S_M = \frac{\int_0^H M(T_{i+1},H)dH - \int_0^H M(T_i,H)dH}{T_{i+1} - T_i}. \quad (2)$$

The calculated $-\Delta S_M(T, H)$ are presented in Figs. 2(d)-2(f). All the curves exhibit a peak feature near T_c. Peaks broads asymmetrically on both sides with increasing field. The maximum of $-\Delta S_M(T, H)$ reach 2.16 J kg^{-1} K^{-1}, 2.11 J kg^{-1} K^{-1}, and 2.03 J kg^{-1} K^{-1} for a, b, and c axis, respectively. It should be noted that all the values of $-\Delta S_M(T, H)$ for easy a axis are positive, however, the values for hard b and c axes are negative at low temperatures in low fields stemming from a strong temperature-dependent magnetic anisotropy.[18]

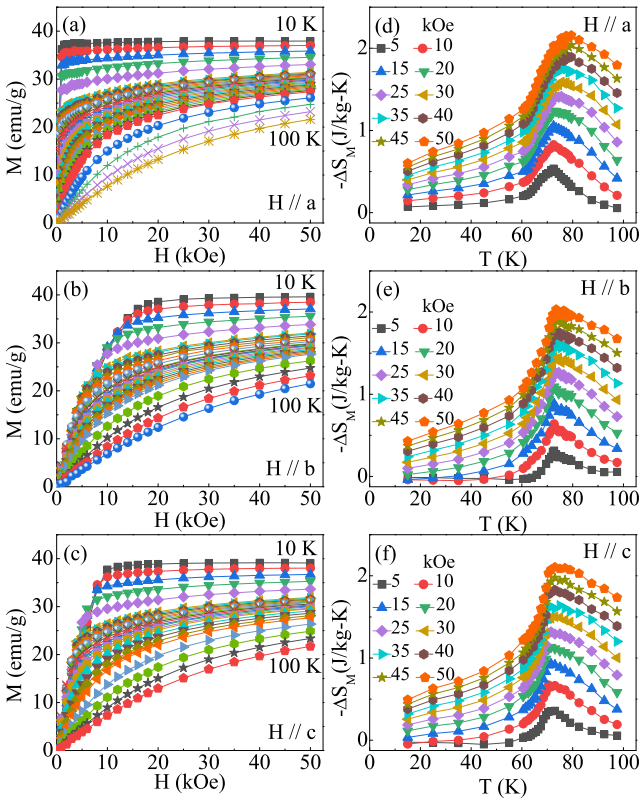

FIG. 2. (Color online). (a-c) Typical initial isothermal magnetization curves measured along all three axes with temperature ranging from 10 to 100 K. (d-f) The corresponding calculated magnetic entropy change $-\Delta S_M(T)$ at various fields change.

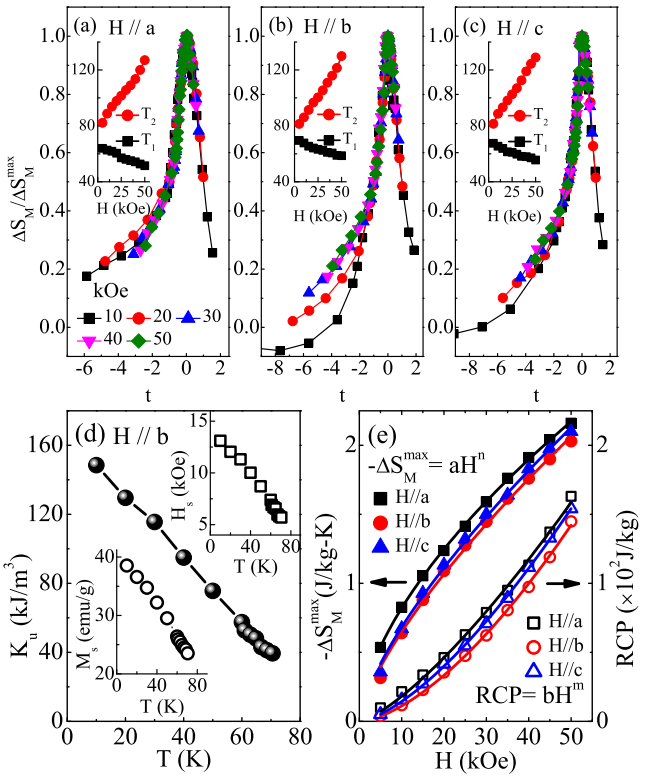

FIG. 3. (Color online). (a-c) Normalized magnetic entropy change ΔS_M as a function of the reduced temperature t along all three principal crystallographic axes of $CrSbSe_3$. Insets show the evolution of the reference temperatures T_1 and T_2. (d) Temperature dependence of the magnetocrystalline anisotropy constant K_u, the saturation field H_s, and the saturation magnetization M_s (insets) estimated from the hard b axis below T_c for $CrSbSe_3$. (e) Field dependence of the maximum magnetic entropy change $-\Delta S_M^{max}$ and the relative cooling power (RCP) with power-law fitting in solid lines along all three axes for $CrSbSe_3$.

Based on a generalized scaling analysis,[27] the normalized magnetic entropy change, $\Delta S_M/\Delta S_M^{max}$, estimated for each constant field, is scaled to the reduced temperature t as defined in the following equations:

$$t_- = (T_{peak} - T)/(T_{r1} - T_{peak}), T < T_{peak}, \quad (3)$$

$$t_+ = (T - T_{peak})/(T_{r2} - T_{peak}), T > T_{peak}, \quad (4)$$

where T_{r1} and T_{r2} are the lower and upper reference temperatures at half-width full maximum of $\Delta S_M/\Delta S_M^{max}$. As we can see, the normalized $\Delta S_M/\Delta S_M^{max}$ near T_c collapses onto a universal curve at the indicated fields for all three axes [Figs. 3(a)-3(c)], indicating the second-order PM-FM transition in $CrSbSe_3$. The ineligible deviation at low temperatures along the hard b axis is mostly contributed by the magnetocrystalline anisotropy effect. Based on the Stoner-Wolfarth model,[28] the magnetocrystalline anisotropy constant K_u can be estimated from the saturation regime in the isothermal magnetization curves. Within this model the value of K_u in single domain state is related to the saturation magnetization M_s and the saturation field H_s with μ_0 is the vacuum permeability:

$$\frac{2K_u}{M_s} = \mu_0 H_s. \quad (5)$$

When $H \parallel b$, the anisotropy becomes maximal. We estimated the M_s by using a linear fit of $M(H)$ above 20 kOe for $H \parallel b$, which monotonically decreases with increasing temperature [inset in Fig. 3(d)]. Then we determined the H_s as the intersection point of two linear fits: one being a fit to the saturated regime at high field, and the other being a fit of the unsaturated linear regime at low field. The values of H_s share a similar temperature dependence [inset in Fig. 3(d)], resulting in a strongly temperature-dependent K_u [Fig. 3(d)]. The calculated K_u is ~ 148.5 kJ m^{-3} at 10 K for $CrSbSe_3$, which is much larger than that of $Cr_2(Si,Ge)_2Te_6$,[18] and comparable with that of $Cr(Br,I)_3$.[21]

Another parameter to characterize the potential magnetocaloric effect of materials is the relative cooling power (RCP):[29]

$$RCP = -\Delta S_M^{max} \times \delta T_{FWHM}, \quad (6)$$

where the FWHM denotes the full width at half maximum of $-\Delta S_M$ curve. The RCP corresponds to the

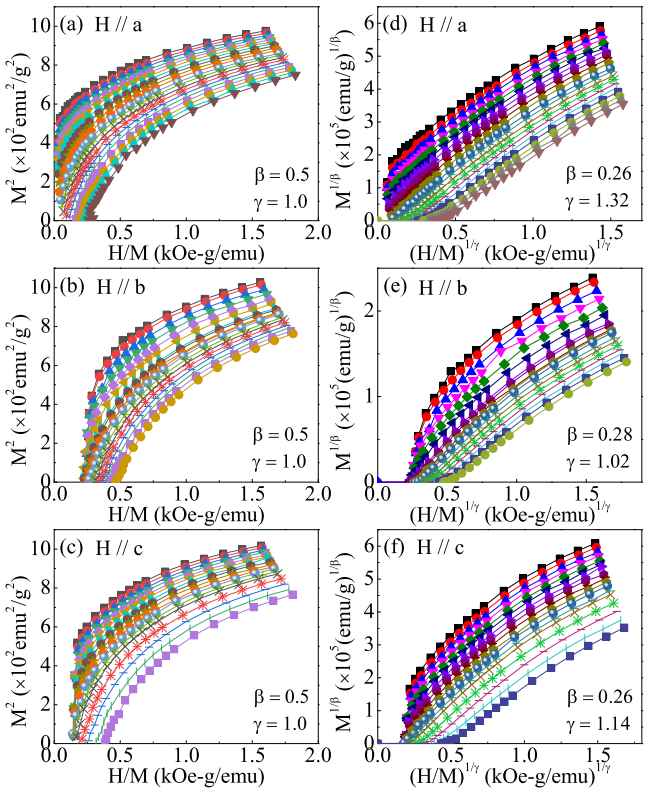

FIG. 4. (Color online). The Arrott plot of M^2 vs H/M (a-c) and the modified Arrott plot of $M^{1/\beta}$ vs $(H/M)^{1/\gamma}$ (d-f) with indicated β and γ for a, b and c axis, repsectively.

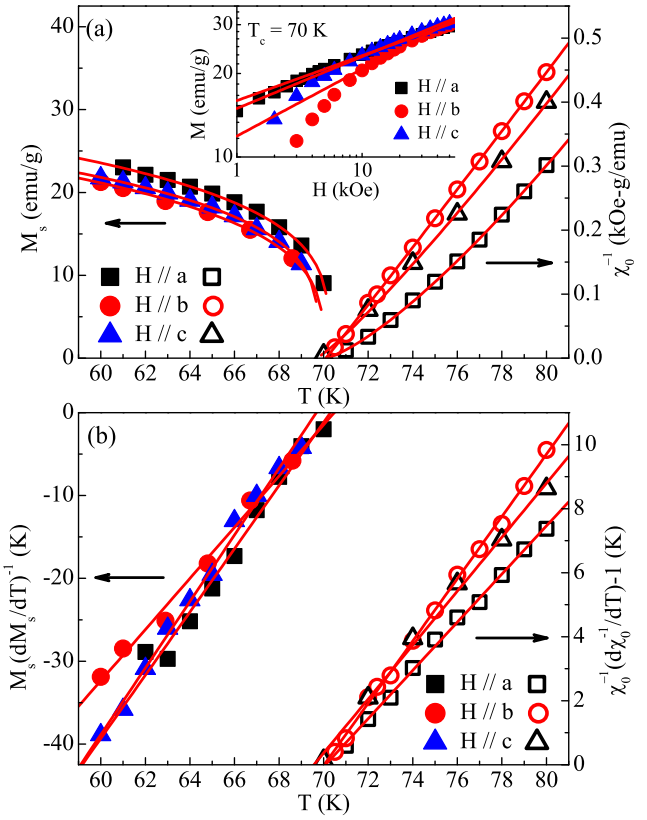

FIG. 5. (Color online). (a) Temperature dependence of the spontaneous magnetization M_s (left) and the inverse initial susceptibility χ_0^{-1} (right) with solid fitting curves for $CrSbSe_3$. Inset shows the $\log_{10}M$ vs $\log_{10}H$ at 70 K with linear fitting curve. (b) Kouvel-Fisher plots of $M_s(dM_s/dT)^{-1}$ (left) and $\chi_0^{-1}(d\chi_0^{-1}/dT)^{-1}$ (right) with solid fitting curves for $CrSbSe_3$.

TABLE I. The values of magnetic entropy change $(-\Delta S_M^{max})$ and relative cooling power (RCP) at field change of 50 kOe. Critical exponents of $CrSbSe_3$ along a, b, and c axis, recpectively. The MAP, KFP, and CI represent the modified Arrott plot, the Kouvel-Fisher plot, and the critical isotherm, respectively.

	$-\Delta S_M^{max}$ (J/kg-K)	RCP (J/kg)	T_c	β	γ	δ
$H \parallel a$	2.16	163.1				
MAP			70.2(1)	0.26(1)	1.32(2)	6.08(12)
KFP			70.2(1)	0.26(1)	1.33(2)	6.12(12)
CI						6.17(9)
$H \parallel b$	2.03	142.1				
MAP			70.1(2)	0.28(2)	1.02(1)	4.64(22)
KFP			70.3(2)	0.32(2)	1.03(1)	4.22(17)
CI						4.14(16)
$H \parallel c$	2.11	154.1				
MAP			69.8(2)	0.26(1)	1.14(5)	5.38(2)
KFP			69.8(2)	0.25(1)	1.19(4)	5.76(2)
CI						5.35(17)

amount of heat which could be transferred between cold and hot parts of the refrigerator in an ideal thermodynamic cycle. The calculated RCP values of $CrSbSe_3$ reach maxima at 50 kOe of 163.1 J kg^{-1}, 142.1 J kg^{-1}, and 154.1 J kg^{-1} for a, b, and c axis, respectively [Fig. 3(e)]. In addition, the field dependence of $-\Delta S_M^{max}$ and RCP can be well fitted by using the power-law relations $-\Delta S_M^{max} = aH^n$ and $RCP = bH^m$ [Fig. 3(e)].[30]

For a second-order PM-FM phase transition, the spontaneous magnetization (M_s) below T_c, the initial magnetic susceptibility (χ_0^{-1}) above T_c, and the field-dependent magnetization (M) at T_c can be characterized by a set of critical exponents β, γ, and δ, respectively.[31] The mathematical definitions of the exponents from magnetization measurement are given below:

$$M_s(T) = M_0(-\varepsilon)^{\beta}, \varepsilon < 0, T < T_c, \quad (7)$$

$$\chi_0^{-1}(T) = (h_0/m_0)\varepsilon^{\gamma}, \varepsilon > 0, T > T_c, \quad (8)$$

$$M = DH^{1/\delta}, T = T_c, \quad (9)$$

where $\varepsilon = (T - T_c)/T_c$; M_0, h_0/m_0 and D are the critical amplitudes.[32] For the original Arrott plot, $\beta = 0.5$ and

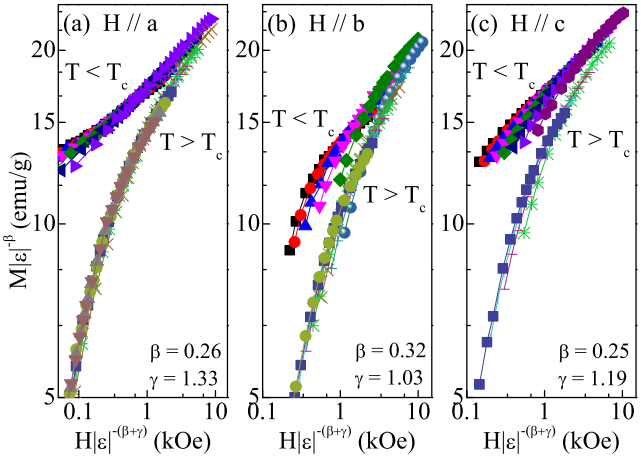

FIG. 6. (Color online). Scaling plots of renormalized $m = M|\varepsilon|^{-\beta}$ vs $h = H|\varepsilon|^{-(\beta+\gamma)}$ above and below T_c for $CrSbSe_3$.

$\gamma = 1.0$.[33] Based on this, the magnetization isotherms M^2 vs H/M should be a set of parallel straight lines. The isotherm at the critical temperature T_c should pass through the origin. As shown in Figs. 4(a-c), all curves in the Arott plot of $CrSbSe_3$ are nonlinear, with a downward curvature, indicating that the Landau mean-field model is not applicable to $CrSbSe_3$. From the Banerjee's criterion,[34] the first (second) order phase transition corresponds to a negative (positive) slope. Thus, the downward slope confirms its a second-order PM-FM transition in $CrSbSe_3$. In the more general case, the Arrott-Noaks equation of state provides a modified Arrott plot:[35]

$$(H/M)^{1/\gamma} = a\varepsilon + bM^{1/\beta}, \tag{10}$$

where $\varepsilon = (T - T_c)/T_c$ and a and b are fitting constants. Figures 4(d-f) present the modified Arrott plots for all three axes with a self-consistent method,[36,37] showing a set of parallel quasi-straight lines at high field.

To obtain the anisotropic critical exponents β, γ and δ, the linearly extrapolated $M_s(T)$ and $\chi_0^{-1}(T)$ against temperature are plotted in Fig. 5(a). According to Eqs. (7) and (8), the solid fitting lines give that $\beta = 0.26(1)$ and $\gamma = 1.32(2)$ for easy a axis, close to the reported values ($\beta = 0.25$ and $\gamma = 1.38$).[8] For the b axis, $\beta = 0.28(2)$ and $\gamma = 1.02(1)$, while for the c axis, $\beta = 0.26(1)$ and $\gamma = 1.14(5)$. This lies between the values of theoretical tricritical mean field model ($\beta = 0.25$ and $\gamma = 1.0$) and 3D Ising model ($\beta = 0.325$ and $\gamma = 1.24$).[38,39] The value of β is outside of the window $0.1 \leq \beta \leq 0.25$ for a 2D magnet,[40] suggesting a 3D magnetic behavior for quasi-1D $CrSbSe_3$. According to Eq. (9), the $M(H)$ at T_c should be a straight line in log-log scale with the slope of $1/\delta$. Such fitting yields $\delta = 6.17(9)$, $4.14(16)$, and $5.35(17)$, for a, b, and c axis, respectively, which agrees well with the calculated values from β and γ based on the Widom relation $\delta = 1+\gamma/\beta$.[41] The self-consistency can also be checked via the Kouvel-Fisher method,[42] where $M_s(T)/(dM_s(T)/dT)^{-1}$ and $\chi_0^{-1}(T)/(d\chi_0^{-1}(T)/dT)^{-1}$ plotted against temperature should be straight lines with slopes $1/\beta$ and $1/\gamma$, respectively. The linear fits to the plots [Fig. 5(b)] yield $\beta = 0.26(1)$ and $\gamma = 1.33(2)$ for a axis, $\beta = 0.32(2)$ and $\gamma = 1.03(1)$ for b axis, $\beta = 0.25(1)$ and $\gamma = 1.19(4)$ for c axis, respectively, very close to the values obtained from modified Arrott plot. All the critical exponents obtained from different methods are listed in Table I. It seems that the critical behavior of $CrSbSe_3$ is much different along the different axis and cannot be described by any single model. However, it is clear that 3D critical behavior dominates in quasi-1D $CrSbSe_3$ and the strong magnetocrystalline anisotropy in $CrSbSe_3$ plays an important role in the origin of anisotropic critical exponents.

Scaling analysis can be used to estimate the reliability of the obtained critical exponents. According to scaling hypothesis, the magnetic equation of state in the critical region obeys a scaling relation can be expressed as:

$$M(H, \varepsilon) = \varepsilon^{\beta} f_{\pm}(H/\varepsilon^{\beta+\gamma}), \tag{11}$$

where f_+ for $T > T_c$ and f_- for $T < T_c$, respectively, are the regular functions. In terms of the variable $m \equiv \varepsilon^{-\beta} M(H, \varepsilon)$ and $h \equiv \varepsilon^{-(\beta+\gamma)} H$, renormalized magnetization and renormalized field, respectively, Eq.(10) reduces to a simple form:

$$m = f_{\pm}(h). \tag{12}$$

It implies that for a true scaling relation with the proper selection of β, γ, and δ, the renormalized m versus h data will fall onto two different universal curves; $f_+(h)$ for temperature above T_c and $f_-(h)$ for temperature below T_c. Using the values of β and γ obtained from the Kouvel-Fisher plot, we have constructed the renormalized m vs h plots in Fig. 6. It is clear seen that all the experimental data collapse onto two different branches: one above T_c and another below T_c, confirming proper treatment of the critical regime.

IV. CONCLUSIONS

In summary, we have studied in details the anisotropic magnetocaloric effect and critical behavior of $CrSbSe_3$ single crystal. The second-order in nature of the PM-FM transition near $T_c = 70$ K has been verified by the scaling analysis of magnetic entropy change ΔS_M. A large magnetocrystalline anisotropy constant K_u is estimated to be 148.5 kJ m^{-3} at 10 K, comparable with that of $Cr(Br,I)_3$. A set of critical exponents β, γ, and δ along each axis estimated from various techniques match reasonably well and follow the scaling equation, indicating a 3D magnetic behavior in $CrSbSe_3$. Further neutron scattering and theoretical studies are needed to shed more light on the anisotropic magnetic coupling in low dimensions.

ACKNOWLEDGEMENTS

This work was supported by the US DOE-BES, Division of Materials Science and Engineering, under Contract No. DE-SC0012704 (BNL).

[1] B. Huang, G. Clark, E. Navarro-Moratalla, D. R. Klein, R. Cheng, K. L. Seyler, D. Zhong, E. Schmidgall, M. A. McGuire, D. H. Cobden, W. Yao, D. Xiao, P. Jarillo-Herrero, and X. D. Xu, Nature **546**, 270 (2017).

[2] M. A. McGuire, G. Clark, KC. S., W. M. Chance, G. E. Jellison, Jr., V. R. Cooper, X. Xu, and B. C. Sales, Phys. Rev. M **1** 014001 (2017).

[3] C. Gong, L. Li, Z. L. Li, H. W. Ji, A. Stern, Y. Xia, T. Cao, W. Bao, C. Z. Wang, Y. Wang, Z. Q. Qiu, R. J. Cava, S. G. Louie, J. Xia, and X. Zhang, Nature **546**, 265 (2017).

[4] M. A. McGuire, H. Dixit, V. R. Cooper, and B. C. Sales, Chem. Mater. **27**, 612 (2015).

[5] N. D. Mermin and H. Wagner, Phys. Rev. Lett. **17**, 1133 (1966).

[6] V. Volkov, G. V. Tendeloo, J. V. Landuyt, S. Amelinckx, E. Busheva, G. Shabunina, T. Aminov, and V. Novotortsev, J. Solid State Chem. **132**, 257 (1997).

[7] D. A. Odink, V. Carteaux, C. Payen, and G. Ouvrard, Chem. Mater. **5**, 237 (1993).

[8] T. Kong, K. Stolze, D. Ni, S. K. Kushwaha, and R. J. Cava, Phys. Rev. Mater. **2**, 014410 (2018).

[9] Y. Sun, Z. Song, Q. Tang, and X. Luo, J. Phys. Chem. C 10.1021/acs.jpcc.0c02101 (2020).

[10] Y. Liu and C. Petrovic, Phys. Rev. B **97**, 014420 (2018).

[11] G. T. Lin, X. Luo, F. C. Chen, J. Yan, J. J. Gao, Y. Sun, W. Tong, P. Tong, W. J. Lu, Z. G. Sheng, W. H. Song, X. B. Zhu, and Y. P. Sun, Appl. Phys. Lett. **112**, 072405 (2018).

[12] Y. Liu and C. Petrovic, Phys. Rev. B **97**, 174418 (2018).

[13] X. Yu, X. Zhang, Q. Shi, S. Tian, H. Lei, K. Xu, and H. Hosono, Front. Phys. **14**, 43501 (2019).

[14] W. Liu, Y. Dai, Yu E. Yang, J. Fan, L. Pi, L. Zhang, and Y. Zhang, Phys. Rev. B **98**, 214420 (2018).

[15] J. Yan, X. Luo, F. C. Chen, J. J. Gao, Z. Z. Jiang, G. C. Zhao, Y. Sun, H. Y. Lv, S. J. Tian, Q. W. Yin, H. C. Lei, W. J. Lu, P. Tong, W. H. Song, X. B. Zhu, and Y. P. Sun, Phys. Rev. B **100**, 094402 (2019).

[16] Y. K. Fu, Y. Sun, and X. Luo, J. Appl. Phys. **125**, 053901 (2019).

[17] Y. Sun and X. Luo, Phys. Status Solidi B 1900052 (2019).

[18] Y. Liu and C. Petrovic, Phys. Rev. Mater. **3**, 014001 (2019).

[19] Y. Liu, J. Li, J. Tao, Y. Zhu, and C. Petrovic, Sci. Rep. **9**, 13233 (2019).

[20] W. Liu, Y. Wang, J. Fan, L. Pi, M. Ge, L. Zhang, and Y. Zhang, Phys. Rev. B **100**, 104403 (2019).

[21] N. Richter, D. Weber, F. Martin, N. Singh, U. Schwingenschlögl, B. V. Lotsch, and M. Kläui, Phys. Rev. Mater. **2**, 024004 (2018).

[22] Y. Liu, L. Wu, X. Tong, J. Li, J. Tao, Y. Zhu, and C. Petrovic, Sci. Rep. **9**, 13599 (2019).

[23] L. D. Casto, A. J. Clune, M. O. Yokosuk, J. L. Musfeldt, T. J. Williams, H. L. Zhuang, M. W. Lin, K. Xiao, R. G. Hennig, B. C. Sales, J. Q. Yan, and D. Mandrus, APL Mater. **3**, 041515 (2015).

[24] S. Selter, G. Bastien, A. U. B. Wolter, S. Aswartham, and B. Büchner, Phys. Rev. B **101**, 014440 (2020).

[25] V. Pecharsky, K. Gscheidner, J. Magn. Magn. Mater. 200, 44 (1999).

[26] J. Amaral, M. Reis, V. Amaral, T. Mendonc, J. Araujo, M. Sa, P. Tavares, J. Vieira, J. Magn. Magn. Mater. **290**, 686 (2005).

[27] V. Franco and A. Conde, Int. J. Refrig. **33**, 465 (2010).

[28] E. C. Stoner and E. P. Wohlfarth, Philos. Trans. R. Soc. Lond. Ser. Math. Phys. Sci. **240**, 599 (1948).

[29] K. A. Gschneidner Jr., V. K. Pecharsky, A. O. Pecharsky, and C. B. Zimm, Mater. Sci. Forum **315**, 69 (1999).

[30] V. Franco, J. S. Blazquez, and A. Conde, Appl. Phys. Lett. **89**, 222512 (2006).

[31] H. E. Stanley, *Introduction to Phase Transitions and Critical Phenomena* (Oxford U. P., London and New York, 1971).

[32] M. E. Fisher, Rep. Prog. Phys. **30**, 615 (1967).

[33] A. Arrott, Phys. Rev. B **108**, 1394 (1957).

[34] S. K. Banerjee, Phys. Lett. **12**, 16 (1964).

[35] A. Arrott, and J. Noakes, Phys. Rev. Lett. **19**, 786 (1967).

[36] W. Kellner, M. Fähnle, H. Kronmüller, and S. N. Kaul, Phys. Status Solidi B **144**, 387 (1987).

[37] A. K. Pramanik, and A. Banerjee, Phys. Rev. B **79**, 214426 (2009).

[38] K. Huang, Statistical Machanics, 2nd ed. (Wiley, New York, 1987).

[39] J. C. LeGuillou, and J. Zinn-Justin, Phys. Rev. B **21**, 3976 (1980).

[40] A. Taroni, S. T. Bramwell, and P. C. W. Holdsworth, J. Phys.: Condens. Matter **20**, 275233 (2008).

[41] B. Widom, J. Chem. Phys. **41**, 1633 (1964).

[42] J. S. Kouvel, and M. E. Fisher, Phys. Rev. **136**, A1626 (1964).